Pharmacological Reports 69 (2017) 813–821

Contents lists available at ScienceDirect

Pharmacological Reports

journal homepage: www.elsevier.com/locate/pharep

Original article

Novel synthetic analogs of diallyl disulfide triggers cell cycle arrest and apoptosis *via* ROS generation in MIA PaCa-2 cells

Vikas Saini[a], Apra Manral[a], Rashi Arora[b], Poonam Meena[a], Siddharth Gusain[a], Daman Saluja[b], Manisha Tiwari[a,*]

[a] Bio-Organic Chemistry Laboratory, Dr. B.R. Ambedkar Centre for Biomedical Research, University of Delhi, Delhi, India
[b] Medical Biotechnology Laboratory, Dr. B.R. Ambedkar Centre for Biomedical Research, University of Delhi, Delhi, India

ARTICLE INFO

Article history:
Received 9 September 2016
Received in revised form 6 February 2017
Accepted 10 March 2017
Available online 14 March 2017

Keywords:
Diallyl disulfide analog
ROS
Apoptosis
Cell cycle arrest
TUNEL
DNA damage

ABSTRACT

Background: Diallyl disulfide (DADS), a principal organosulfur component of garlic, is known for its medicinal properties including anti-cancer activity. Prior studies have demonstrated that the compounds containing Diallyl disulfide moieties exhibited diverse therapeutic potential with promising biological activities. In the present study, we have investigated the *in vitro* anticancer activity of Diallyl disulfide derivatives (5a–5 l and 7e-7m) against human cancer cell lines.
Methods: The effect of DADS analogs on different cancer cell lines was measured through MTT assay. Cell cycle progression, apoptosis, DNA fragmentation and levels of ROS were analyzed through FACS and confocal imaging.
Results: Bis[3-(3-fluorophenyl)prop-2-ene]disulfide (compound 5b) was the most potent compound among the tested DADS derivatives. FACS analysis revealed that increase in ROS generation by compound 5b was accompanied by cell cycle arrest in the G2/M phase and apoptosis in MIA PaCa-2 cells. Further, the apoptosis was confirmed by TUNEL assay. Western blot analysis showed that compound 5b induces G2/M phase arrest *via* ROS mediated DNA-damage, which in turn, induces phosphorylation of Chk1/Cdc25c/Cdc2 pathway. Furthermore, altered levels of ROS triggers intrinsic apoptotic cascade, as evidenced by dissipated mitochondrial membrane potential (ψ), decrease in Bcl-2/Bax ratio, cytochrome c release and cleavage of procaspase-3. Scavenging of ROS by antioxidant *N*-acetyl-cysteine (NAC) reversed the compound 5b induced augmented intracellular ROS levels and cell death.
Conclusion: Taken together, the anti-proliferative effects of compound 5b were attributed to intracellular ROS accumulation, which in turn, triggers apoptosis by mediating DNA damage-induced G2/M phase arrest and evoking mitochondrial apoptotic pathway in MIA PaCa-2 cells.

Introduction

Cancer is one of the main causes of death worldwide; with 14.1 million new cases and 8.2 million deaths in 2012, according to the worldwide cancer statistics [1]. Chemotherapy is still one of the primary regimens for the treatment of cancer. However, the use of available chemotherapeutics is often limited mainly due to toxicities and drug resistance. Therefore, identifying potent antitumor agents with novel scaffolds are critically desired.

Oxidative stress plays an important role in controlling cancer cell behavior. Due to their accelerated metabolism, cancer cells exhibit higher ROS levels compared to normal cells, turning them more susceptible to oxidative stress-induced cell death [2]. Therefore, many chemotherapeutic strategies are designed to overwhelming raise ROS levels, with the aim to induce irreparable damages eventually resulting in tumor cell apoptosis [3].

Diallyl disulfide, a major organosulfur derived from garlic, is well known to exhibit pharmacological activities against various diseases, including the anti-cancer activity against various types of human cancer cells such as breast [4], lung [5] and colon [6] cancer cells. However, potential use of diallyl disulfide is limited due to its highly volatile nature and low bioavailability. Therefore, to supersede this problem; our laboratory took interest in the synthesis of substituted DADS derivatives which demonstrated greater stability along with potent pharmacological activities [7–11].

The present study describes *in vitro* evaluation of anti-proliferative activity of previously reported series of novel DADS

* Corresponding author.
E-mail address: mtiwari07@gmail.com (M. Tiwari).

http://dx.doi.org/10.1016/j.pharep.2017.03.006
1734-1140/

derivatives (5a-5l and 7e-7m) [7] against human pancreatic cancer cells, MIA PaCa-2; human cervical cancer cells, HeLa; human liver cancer cells, HepG2; and normal human embryonic kidney cells, HEK 293 cells. The most potent compound Bis[3-(3-fluorophenyl) prop-2-ene]disulphide (5b), as shown in Fig. 1(b), was selected from the 21 tested DADS analogs. Furthermore, to determine the anti-cancer action of compound 5b, its effects on ROS generation, cell cycle progression and apoptotic signaling pathways on pancreatic cancer cells, MIA PaCa-2 was examined.

Materials and methods

Chemicals and reagents

MTT, Trypan blue, Tris-HCl, Triton X-100, H_2DCFDA, Propidium iodide (PI), ribonuclease-A and *N*-acetyl cysteine (NAC) were obtained from Sigma Chemical Co. (St. Louis, USA). Potassium phosphates, *p*-formaldehyde and dimethyl sulfoxide (DMSO) were purchased from Merck Co. (Darmstadt, Germany). Penicillin-streptomycin, trypsin-EDTA and fetal bovine serum (FBS) were obtained from Himedia (Mumbai, India). The JC-1 assay and Annexin-V/APC kit was purchased from BD biosciences (San Jose, CA, USA) and e-biosciences (San Diego, USA), respectively

Cell culture conditions and DADS analogs treatment

All the cell lines were obtained from National Centre for Cell Sciences (NCCS, India). Cells were cultured in the Dulbecco's Modified Eagle medium supplemented with 10% fetal bovine serum at 37 °C in 5% CO_2 atmosphere. All twenty-one DADS derivatives were synthesized by scheme previously standardized by our group [7]. DADS derivatives were dissolved in DMSO followed by serial dilution in PBS and the final DMSO concentration in all cultures was less than 0.3%.

Cell viability analysis and morphological changes

Cell viability analysis was carried out by colorimetric 3-(4,5-dimethylthiazol-2-yl)-2,5-diphenylthiazolbromide (MTT) assay. Cells were seeded at a plating density of 2000/well and treated with different concentrations (100 nM to 200 μM) of DADS analogs. The final concentration of DMSO in the culture medium was found to have no cytotoxic effect on either cell line. Following treatment with different compounds for 48 h, MTT (Sigma) was added, and the absorbance of samples was measured at 565 nm using Tecan Infinite M200 plate reader. IC_{50}, the concentration of compound required to inhibit 50% cell growth, was determined by plotting a graph of Log (concentration of compound) *vs.*% cell viability. Calculation of IC_{50} value was done using GraphPad Prism Software (Ver. 5.01). The assay was performed three times and the results are given as mean ± SEM of independent experiments.

Cell cycle arrest

Measurement of the relative DNA content of the cells was performed by FACS analysis. Briefly, MIA PaCa-2 and HeLa cells were incubated with compound 5b (IC_{50} = 7.23 μM) for different time intervals and then harvested, fixed in 70% ethanol (in PBS), kept overnight at 4 °C. Further, cells were resuspended in PBS, incubated with 1 mg/ml of RNase for 30 min at 37 °C, followed by incubation with propidium iodide (PI) (20 μg/ml) for 20 min. Fraction of cells in different phases of cell cycle (10,000 events/sample) were quantified using Cell Quest pro software. Results are expressed as the mean ± SEM of three independent experiments.

Annexin-V (APC)/propidium iodide dual staining assay

Mode of cell death was examined using Annexin V Apoptosis Detection kit APC (e-Biosciences), as per the manufacturer's protocol. Briefly, MIA PaCa-2 and HeLa cells were treated with compound 5b for different time intervals at its IC_{50} value of 7.23 μM. Cells were harvested, resuspended in 1X binding buffer, incubated with Annexin V-APC and PI stain for 20 min at 37 °C. 10,000 events/sample were taken and data were acquired using logarithmic amplification of FL4 (APC) and FL2 (PI) channels using BD FACSCALIBUR™, and further analyzed by Cell Quest pro software. Results are expressed as the mean ± SEM of three independent experiments.

Measurement of intracellular ROS accumulation

The levels of ROS from MIA PaCa-2 cells were examined and determined by FACS using 2′,7′-dichlorodihydrofluorescein diacetate (H_2DCFHDA, Sigma) for staining as previously described [12].

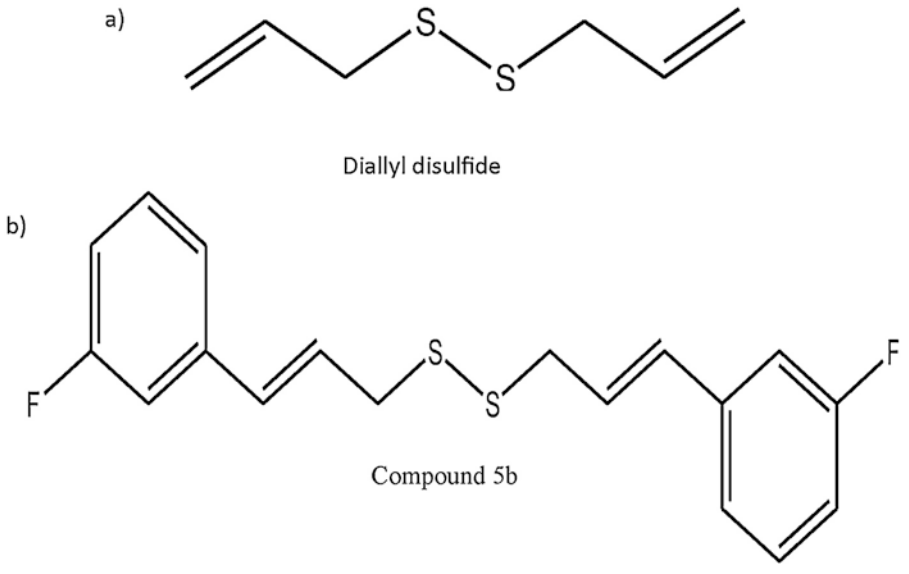

Fig 1. Chemical Structure of (a) Diallyl disulfide (DADS) (b) Structure of Bis[3-(3-fluorophenyl)prop-2-ene]disulphide (5b).

Briefly, cells were treated with compound 5b at its IC_{50} for different time intervals to detect the changes in ROS. The cells were harvested and washed twice, re-suspended in 500 μM of H_2DCFHDA solution (10 μM stock), incubated at 37 °C for 30 min and analyzed by FACS (10,000 events/sample). Results are expressed as the mean ± SEM of three independent experiments.

Effect on mitochondrial membrane potential ($\Delta\Psi_m$)

Effect of compound 5b on mitochondrial membrane potential was measured using the JC-1 dye (5,5′,6,6′-tetraethylbenzimidazolecarbocyanine iodide) following manufacturer's instructions (BD™ MITOSCREEN (JC-1)). Briefly, after the desired treatments for 12 and 24 h, cells were harvested, washed twice with PBS and then incubated at 37 °C for 20 min with staining buffer containing JC-1. After incubation, cells were washed with staining buffer twice and data were acquired (10,000 events/sample) using BD FACSCALIBUR™ and analyzed by Cell Quest pro software. The green and red fluorescence ratio measured the proportion of mitochondrial depolarization. Results are expressed as the mean ± SEM of three independent experiments.

DNA gel electrophoresis

MIA PaCa-2 cells (1×10^6 cells/well) seeded in 6-well plates were treated with compound 5b for 48 h. Cells were harvested and DNA was extracted from cells using DNA isolation kit (Qiagen Technology). The extracted DNA samples were electrophoresed on a 1.5% agarose gel in Tris-acetic acid-EDTA buffer. After electrophoresis, the gel was stained with ethidium bromide (EtBr, Sigma-Aldrich Corp.) and the bands obtained were visualized using a UV light transilluminator.

TUNEL assay

Confocal microscopy was performed to observe morphological nuclear DNA fragmentation in the MIA PaCa-2 cells using DeadEnd™ fluorometric TUNEL system, following the manufacturer's protocol (Cat# G3250, Promega, USA). Briefly, MIA PaCa-2 cells were seeded over slides and after the required treatments, slides were fixed with 4% formaldehyde in PBS, followed by permeabilization with 0.2% Triton® X-100 and labelling with TdT reaction mix. DAPI (4′,6-diamidino-2-phenylindole) (Vector Lab Cat. # H-1200) was used to stain nuclei. Confocal imaging was performed with Nikon C2 laser scan confocal microscope with 60 x objective magnification, numerical aperture 1.4, refractive index 1.5, Plan Apo optics equipped with an argon laser, using excitation and emission wavelength of 490 and 525 nm respectively for FITC and 461 and 500 nm respectively for nuclear stain DAPI. Data was analyzed using the NIS Elements AR software.

Further, to quantitate the nuclear DNA fragmentation, FACS analysis was performed in the MIA PaCa-2 cells using the same TUNEL system, following the manufacturer's protocol. DNase was used as a positive control as previously described [13]. The fluorescein-12-dUTP labeled DNA was quantitated by Cell Quest pro software by measuring the green fluorescence (FL1) at 520 nm using BD FACSCALIBUR™. The experiment was performed thrice and the results were given as mean ± SEM of independent experiments.

Western blot analysis

MIA PaCa-2 cells (2×10^6 cells) were treated with the compound 5b (7.23 μM) for 6, 12, 24 and 48 h and cell pellets were extracted with RIPA buffer (Cell Signaling Technology, MA, US) with EDTA-free protease inhibitor containing phosphatase inhibitors such as sodium orthovanadate and sodium pyrophosphate in the cocktail (Santa Cruz, USA). Protein quantification was done using commercial protein estimation BCA™ kit (Bangalore Genei). Equal amounts of protein (30–50 μg) were loaded, resolved on a 10–12% SDS–Polyacrylamide gel and transferred to a PVDF membrane, blocked with 5% Bovine serum albumin protein for 2 h at room temperature. The membrane was incubated overnight at 4 °C with primary antibodies (1:1000-1:2000), followed by incubation with horseradish peroxidase–conjugated secondary antibodies (1:5000-1:10000) for 3 h at room temperature. Immunoreactive bands were probed with the enhanced chemiluminiscence (ECL) western blot detection system (Biogene, India) according to manufacturer's instructions and viewed in gel documentation system LAS4000 (FUJIFILM, USA). All the bands were quantitated by ImageJ software and normalized to vehicle controls and the results were given as mean ± SEM of three independent experiments. Antibodies against caspase-3 (sc-7272), cytochrome-c (sc-13156), Bax (sc-7480), Bcl-2 (sc-7382), Cdc25C (sc-13138), p-Cdc2 (sc-7989), Cyclin B1 (sc-25764) and β-actin (sc-130301) were purchased from Santa Cruz (USA). Antibodies against cleaved caspase-3 (#9661), Chk-1 (#2360), p-Chk1 (#2348), and p-Cdc25C (#4901), were purchased from Cell Signaling Technology, Inc.

Statistics

Data are presented as mean ± SEM. The intergroup variation was measured by one-way analysis of variance (ANOVA) followed by Tukey *post-hoc* test, in which $p < 0.05$ was considered to be statistically significant. Statistical studies were performed using Graph Pad Prism Software 5.0.

Results

Cell viability analysis

The effect of DADS analogs 5a-l and 7e-m were studied against normal human embryonic kidney cells (HEK-293) and three cancer cell lines: MIA PaCa-2 (Human pancreatic cancer cell line), HepG2 (Human hepatic cancer cells) and HeLa (Human cervical cancer cells) using MTT assay. The potencies of the compounds were expressed as the half maximal inhibitory concentration (IC_{50}), summarized in Table 1. The most potent compound Bis[3-(3-flourophenyl) prop-2-ene] disulfide (5b), among the 21 tested analogs, exhibited nearly similar activity against both HepG2 (IC_{50} = 27.9 μM) and HeLa (IC_{50} = 26.6 μM) cell lines. However, the IC_{50} values of compound 5b (7.23 μM) against MIA PaCa-2 were three to fourfold lower as compared to the other two cancer cell lines (supplementary Fig. S1). Henceforth, all the assays were carried out on MIA PaCa-2 cells with compound at its IC_{50} of 7.23 μM. In addition, the IC_{50} value of DADS was found to be 280, 242 and 155 μM for MIA PaCa-2, HepG2 and HeLa cell lines, respectively. Furthermore, phase contrast micrographs of compound 5b treated cells showed loss of cell morphology, de-adherence tendency and cell shrinkage instead of spreading along with proliferation (Supplementary Fig. S2).

Annexin-V (APC)/propidium iodide dual staining assay

To elucidate the mechanism of cell death by compound 5b, Annexin-V APC/PI dual staining assay was performed. As illustrated in Fig. 2A, compound 5b could efficiently induce apoptosis in MIA PaCa-2 cells in a time dependent manner at its IC_{50} value. It was observed that compound 5b treatment increased the majority of MIA PaCa-2 cells in the early apoptotic stage (6.34%, 11%, 23.50% and 38.33%) and late apoptotic stage (19.81%, 21.61%,

Table 1
Shows IC_{50} value of Diallyl disulfide analogs on pancreatic cancer cell line (MIA PaCa-2), Hepatic cancer cell line (HepG2), Human cervical cancer cell line (HeLa) and Human embryonic kidney cell line (HEK).

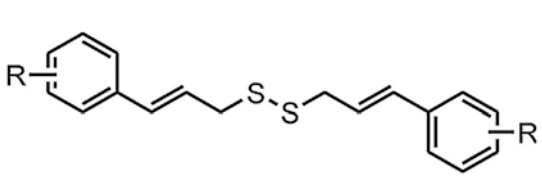

(5a-5l)

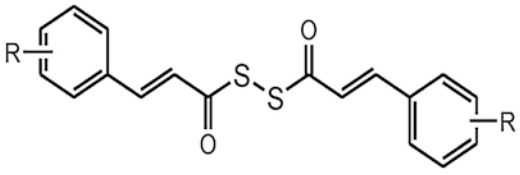

(7e-7m)

Compound	Substituent 'R'	IC_{50} (μM)[b]			
		MIA PaCa−2[a]	HepG2[a]	HeLa[a]	HEK[a]
5a	R = 2-F	52.5 ± 2.08	75 ± 3.04	53.3 ± 1.12	>100
5b	R = 3-F	7.23 ± 1.04	27.07 ± 1.3	26.36 ± 0.32	>100
5c	R = 3-Cl	46.09 ± 1.96	67.5 ± 2.32	39.81 ± 0.75	>100
5d	R = 3,5- diCl	58.44 ± 1.52	56 ± 1.16	43.53 ± 1.02	>100
5e	R = 2,6-diF	43.3 ± 3.36	52.5 ± 2.09	38.52 ± 2.11	92.5 ± 2.65
5f	R = 4-Cl	25 ± 2.53	38 ± 1.86	32.27 ± 2.71	82.9 ± 1.29
5g	R = 3-Br	83.13 ± 4.12	87.5 ± 2.84	54.82 ± 1.57	>100
5h	R = 4-Br	90.2 ± 4.56	80 ± 3.22	92.31 ± 1.76	>100
5i	R = 4-OH	>100	>100	91.62 ± 1.34	>100
5j	R = 4-OCH_3	78.1 ± 3.15	>100	82.91 ± 1.26	>100
5k	R = 3,4-diOCH_3	72.05 ± 3.22	87.5 ± 2.84	>100	>100
5l	R = 4-OH, 3-OCH_3	95 ± 4.56	>100	>100	>100
7e	R = 4-F	51.07 ± 2.51	55.5 ± 2.32	60.89 ± 1.14	>100
7f	R = 4-Cl	63.59 ± 3.62	54.6 ± 1.25	78.63 ± 2.51	>100
7g	R = 3-Br	82.36 ± 2.84	75 ± 2.65	66.80 ± 1.29	>100
7h	R = 4-Br	77.4 ± 2.35	>100	>100	>100
7i	R = 4- OH	78.01 ± 2.65	93.5 ± 2.32	>100	>100
7j	R = 4-OCH_3	98 ± 1.14	>100	>100	>100
7k	R = 3,4-diOCH_3	>100	>100	>100	>100
7l	R = 4-OH, 3-OCH_3	>100	>100	>100	>100
7m	R = 2,4-diOCH_3	>100	>100	>100	>100
Doxorubicin[c]		0.43 ± 0.036	0.15 ± 0.02	0.09 ± 0.02	0.59 ± 0.01
DADS		242 ± 1.05	280 ±1.93	155 ± 2.6	–

[a] Cell lines were treated with different concentrations of the compounds for 48 h. Cell viability was measured by MTT assay as described in the experimental section.
[b] IC_{50} values are indicated as Mean ± S.D of three independent experiments.
[c] Doxorubicin was taken as positive control.

21.58% and 43.90%), at time intervals of 6, 12, 24 and 48 h, respectively, in comparison to untreated control cells where only 0.55% and 1.68% of cells were found in early and late apoptotic stage, respectively. These results demonstrated that compound 5b effectively induced cell apoptosis in MIA PaCa-2 cells in a time-dependent manner, eventually leading to cell death.

Detection of DNA fragmentation by TUNEL assay

To further consolidate our findings that compound 5b treated MIA PaCa-2 cells shows late apoptotic characteristic, detection of DNA fragmentation was examined by DAPI/TUNEL double staining assay and monitored by confocal imaging and TUNEL labelling by FACS analysis. As shown in Fig. 3A(j), an increase in intensity of green fluorescence was observed after treatment with compound 5b for 48 h, as compared to untreated control cells which emitted only blue fluorescence indicating the presence of healthy cells (Fig. 3A(a–d)). In positive control, brief treatment of DNase for 1 h in MIA PaCa-2 cells induced DNA fragmentation as indicated by increase in intensity of green fluorescence (Fig. 3A (e–h)). However, the cells treated with compound 5b for 48 h revealed nuclear condensation and formation of apoptotic bodies, which was typical of late apoptosis (as indicated by the arrows in Fig. 3A(j–i)).

Also, quantification of DNA fragmentation by FACS analysis showed an increase in fluorescence intensity in compound 5b treated cells (79.58%) as compared to control (20.63%) (Fig. 3B and C).

Further, a typical DNA ladder analysis was performed in MIA PaCa-2 cells for 48 h at its IC_{50}. The chromosomal DNA was extracted from MIA PaCa-2 cells and used for agarose gel electrophoresis. The results from Fig. 3D indicated that 5b induces DNA fragmentation in MIA PaCa-2 treated cells, which lead to a significant ladder pattern of internucleosomal DNA fragmentation in gel lane D with respect to untreated control (Lane B), where intact DNA was observed. However, in case of positive control, DNase (Lane C), a smear was observed indicating excessive DNA fragmentation, validating our findings of TUNEL assay.

Effect of compound 5b on apoptotic markers

To further examine the mechanism of compound 5b-induced apoptosis, the effects of 5b on the protein expression of Bax, Bcl-2, total cytochrome-c and caspase-3, which are important apoptosis-associated proteins, were examined. MIA PaCa-2 cells were treated with compound 5b for 6, 12, 24 and 48 h and their expression levels were determined by western blot analysis. As shown in Fig. 2B, compound 5b treatment induced a time dependent up-regulation in the levels of pro-apoptotic protein Bax with a concomitant decline in the levels of anti-apoptotic protein Bcl-2 as compared to control group. The decrease in Bcl-2/Bax proteins disrupts MMP triggering the release of cytochrome c from mitochondrial

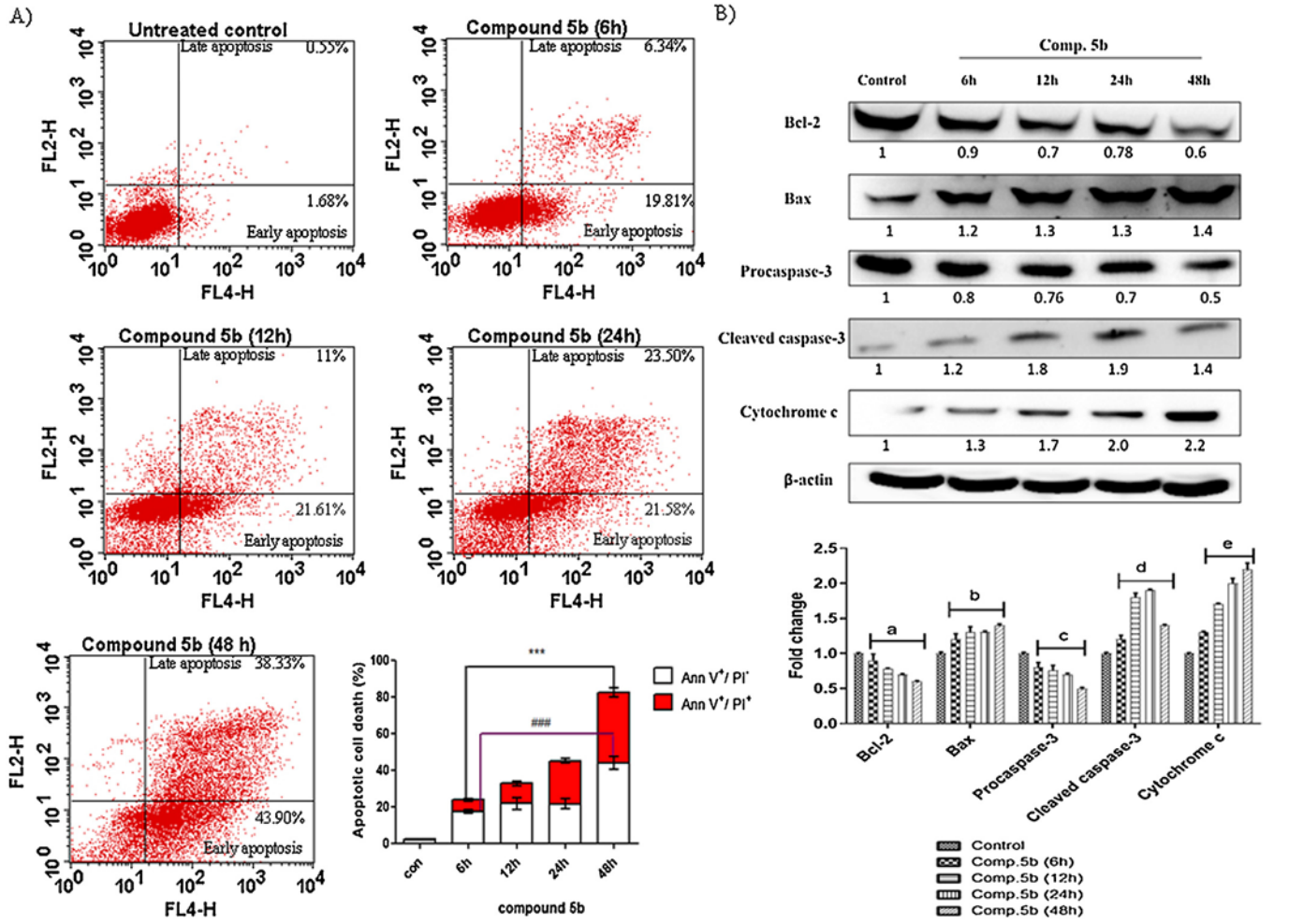

Fig. 2. Compound 5b induces apoptosis in MIA PaCa-2 cells (A) FACS analysis for the detection of apoptosis by Annexin-V (APC)/PI double staining assay in MIA PaCa-2 cells, treated with comp 5b for 6, 12, 24 and 48 h. Graph bars represents percentage of cells in the early and late apoptotic stages (mean ± SEM, $n = 3$). $^{\#\#\#}p < 0.001$ *vs.* control (Annexin-V^+/PI^-); $^{***}p < 0.001$ *vs.* control (Annexin-V^+/PI^+). (B) Effect of compound 5b on the expression levels of proteins associated with mitochondrial dependent apoptotic pathway at different time intervals in MIA PaCa-2 cells by western blot analysis. β-actin was used as loading control (mean ± SEM, $n = 3$). Significant differences from respective controls are as follows: $^a p < 0.001$; $^b p < 0.001$,$^c p < 0.001$; $^d p < 0.001$ and $^e p < 0.001$.

membrane into the cytoplasm. From Fig. 2B, it was evident that compound 5b treatment induced cytochrome c accumulation in cytoplasm followed by decline in the levels of inactive procaspase-3 and increased expression of its active form *i.e.* cleaved caspase-3 in a time dependent manner. The presence of active caspase-3 marked the execution of apoptotic cascade.

Effect on mitochondrial membrane potential ($\Delta\Psi_m$)

To further understand how the compound 5b induced the apoptotic signaling pathway, the changes in mitochondrial membrane permeability (MMP) were initially detected. In MIA PaCa-2 cells treated with compound 5b at IC_{50} concentration for 12 and 24 h, MMP was reduced in a time dependent manner as indicated by red/green fluorescence (Fig. 4A). As shown in the histogram, there was a remarkable shift in the green fluorescence that increased to 37.43% and 67.73% in 12 and 24 h, respectively, as compared to control cells.

Compound 5b increased intracellular ROS levels, and NAC reversed compound 5b-induced ROS generation and cell death

To determine whether the cell apoptosis induced by compound 5b is ROS dependent, we evaluated the intracellular ROS generation in MIA PaCa-2 cells. As shown in Fig. 4C, untreated control cells generate low levels of intracellular ROS, as reflected by corresponding low DCF fluorescence intensity. In contrast, cells treated with compound 5b (7.23 μM) for 3, 6 and 12 h showed an increase in intensity of the green fluorescence from 3 to 6 h followed by a decrease in 12 h. As shown in Fig. 4C, intracellular ROS generation increased to 60.6% and 84.6% in 3 and 6 h, respectively, which further decreased to 66.4% after 12 h. In the positive control, MIA PaCa-2 cells incubated with 100 μM H_2O_2 for 6 h generated high intracellular ROS (94%), which was comparable to compound 5b at 6 h. However, pre-treatment with NAC (5 mM) for 1 h, significantly reduced 5b-induced ROS generation (Fig. 4C) and cell death (Fig. 4D).

Cell cycle analysis

To further examine the anti-proliferative effect of compound 5b, we examined DNA distribution of cells into different phases of the cell cycle at different time intervals of 6, 12, 24 and 48 h in MIA PaCa-2 cells (IC_{50} = 7.23 μM) by propidium iodide staining using FACS. As revealed by DNA histograms in Fig. 5A, an increase in accumulation of cells in G2/M phase in a time dependent manner where the increase in cell population were found to be 24.30%, 34.30% and 63.59% in 6, 12 and 24 h, respectively, which was

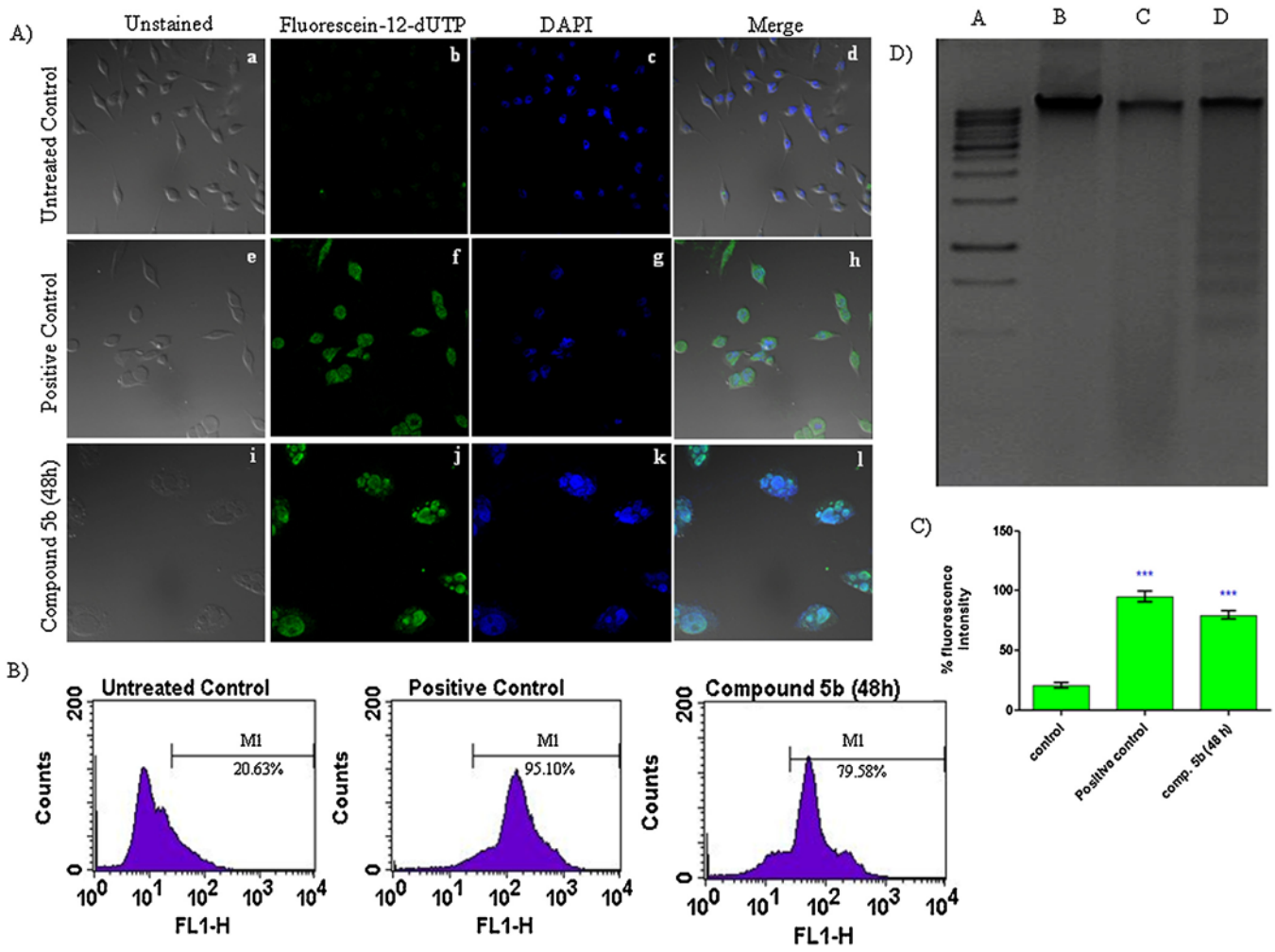

Fig. 3. (A) Confocal images of MIA PaCa-2 cells stained with fluorescein-12-dUTP (green) and counterstained with DAPI (blue). (a–d) Untreated control cells without green fluorescence represents intact DNA; (e–h) DNase was used as a positive control, showing fragmented DNA; (i–l) MIA PaCa-2 cells treated with compound 5b for 48 h, arrows indicating fragmented DNA and formation of large vacuolated apoptotic bodies. (B) FACS quantification of compound 5b induced DNA fragmentation in MIA PaCa-2 cells. (C) The bar graph displays the percentage of cells labeled with fluorescein-12-dUTP staining (mean ± SEM, $n = 3$), $^{***}p < 0.001$ *vs.* untreated control. (D) Compound 5b induced DNA fragmentation. Lane A, 1 Kb ladder; Lane B, Untreated control; Lane C, positive control (DNase); Lane D, Compound 5b treatment for 48 h. (For interpretation of the references to colour in this figure legend, the reader is referred to the web version of this article.)

comparatively higher as compared to untreated control (17.27%) indicating a G2/M-phase arrest. However, after 48 h, there was an increase in percentage of cells in the sub-G1/G0 peak reflecting cell population undergoing apoptosis.

Effect of compound 5b on cell cycle regulatory protein

To further validate the anti-proliferative activity of compound 5b was mediated by cell cycle arrest, the expression analysis of various G2/M phase associated regulatory proteins was analyzed by western blotting. In the current studies, compound 5b-induced up-regulation in the expression of phosphorylated-Chk1 (p-Chk1) protein in MIA PaCa-2 cells in a time-dependent manner. As shown in Fig. 5B, the increase in p-Chk1 was accompanied by an up-regulation of inactive phosphorylated Cdc25C protein and simultaneously marked reduction in Cdc25C expression. The accumulation of p-Cdc25C protein, in turn failed to remove phosphate group from Cdc2 protein as indicated by presence of elevated levels of phospho-Cdc2 in a time dependent manner.

Discussion

The anti-cancer potency of DADS has been studied for many years through *in vitro* and *in vivo* studies [14,15]. However, its use as a therapeutic agent is restricted due to its unstable and highly volatile nature. Previous studies in our laboratory have reported the synthesis of substituted derivatives of DADS with greater stability and efficacy than the parent compound DADS [7,9]. In the present study, we have demonstrated the anti-proliferative effect of DADS analogs and explored their mechanism of action.

Our experiment revealed potent inhibitory activity of DADS derivatives against MIA PaCa-2 cancer cells and modest activity against HepG2 and HeLa cancer cells. It was observed that between the two series, derivatives from first series (5a-5l) displayed higher potency than their counterparts from second series (7e-7m). The trend obtained within the two series revealed that compounds bearing electron withdrawing substituents (–F > –Cl > –Br) exhibited better activity than their electron donating counterparts (–OH, $–OCH_3$) suggesting the influence of electronic nature of substituents on the potencies of the compounds. The introduction of

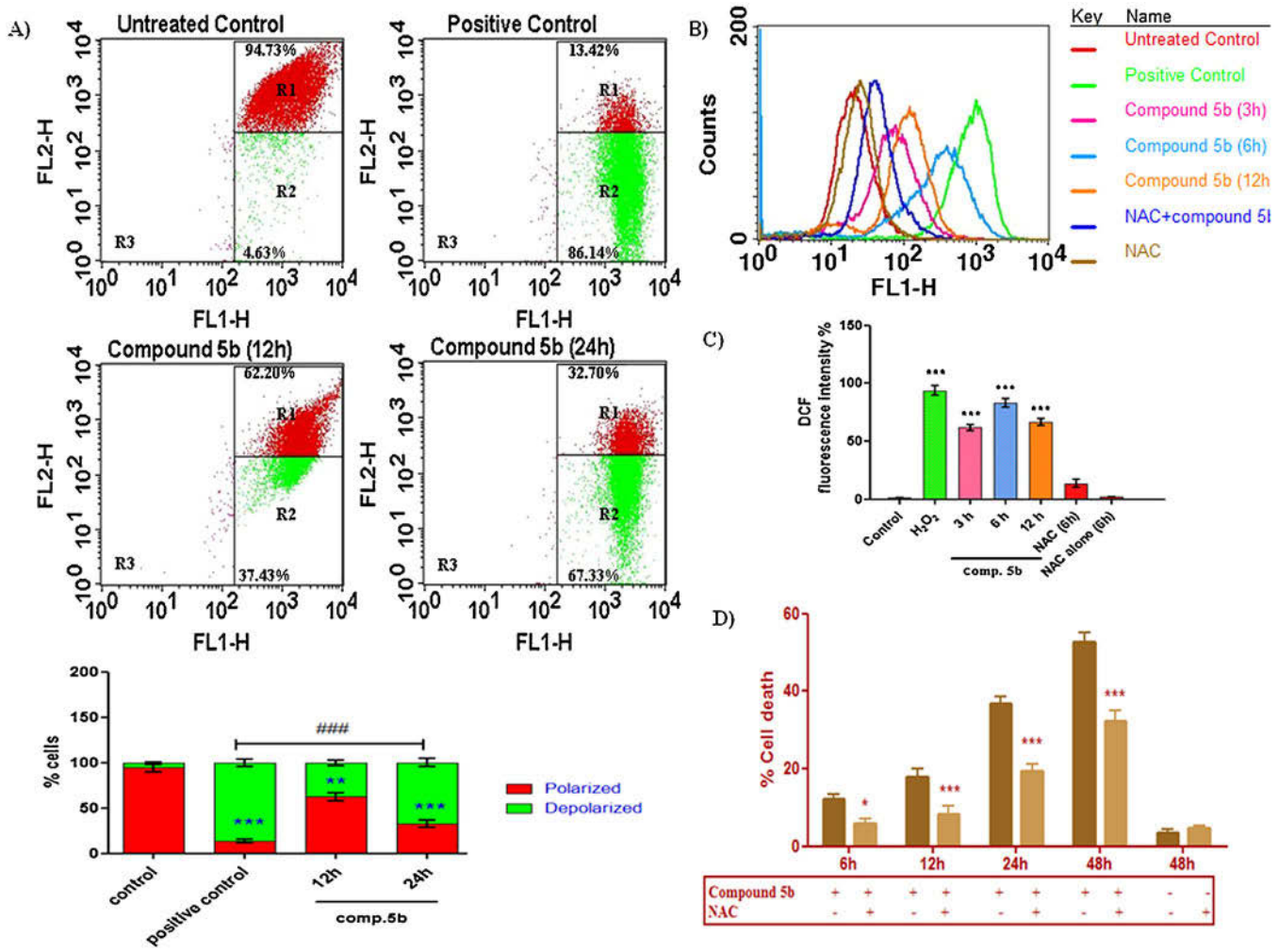

Fig. 4. (A) Effect of comp 5b on the mitochondrial membrane potential of MIA PaCa-2 cells after 12 and 24 h of treatment. Cells treated with CCCP were taken as positive control. The bar graph displays the percentage of cells with depolarized mitochondria (mean ± SEM, $n = 3$); Significant differences from respective controls: $^{\#\#\#}p < 0.001$; $^{**}p < 0.01$ and $^{***}p < 0.001$. (B–D) Compound 5b induced cell death was mediated by ROS (B) MIA PaCa-2 cells were incubated with H_2DCF-DA, treated with compound 5b for 3, 6 and 12 h with or without 2 h pretreatment of NAC (5 mM), examined for ROS production by FACS. Cells treated with 100 μM H_2O_2 for 30 min were taken as positive control. (C) Quantification of ROS production represented in terms of DCF fluorescence intensity is shown as bar graph (mean ± SEM, $n = 3$); $^{***}p < 0.001$ *vs.* untreated control. (D) Cell viability was evaluated in MIA PaCa-2 cells on treatment with compound 5b alone or in the presence of NAC (5 mM) for 6, 12, 24 and 48 h using MTT assay. Data represent the mean of three measurements ± SEM, n = 3. $^{*}p < 0.05$ and $^{***}p < 0.001$ *vs.* respective time controls.(For interpretation of the references to colour in the text, the reader is referred to the web version of this article.)

3-Fluoro substituent on phenyl ring (compound 5b) afforded the most efficacious analog. On the basis of preliminary cell viability studies, the IC_{50} of compound 5b was achieved at 7.23–27.07 μM whereas the IC_{50} of DADS was in the range of 155–280 μM, which clearly indicated that DADS analogs were more potent than the parent compound DADS. Inspired by the promising preliminary *in vitro* results, Bis[3-(3-flourophenyl) prop-2-ene] disulfide (compound 5b) was chosen to explore the mechanism of anti-proliferative action against the MIA PaCa-2 cell line. In addition, corresponding anti-proliferative and apoptotic activity of compound 5b was also checked on other cell line such as HeLa, and similar results were obtained but at higher concentration (IC_{50} = 26.36 μM) than MIA PaCa-2 (Supplementary Figs. S3, S4). The observed higher selectivity of compound 5b towards MIA PaCa-2 cells could be due to difference in the doubling time among the cancer cell lines or by differential intrinsic ability of cancer cells to respond to various chemotherapeutic agents. HeLa cells have a shorter doubling time of 24 h as compared to MIA PaCa-2 and HepG2 cells, which doubles their cell number in 48 h and 40 h, respectively. The difference in time period of cell cycle progression could affect the sensitivity of cells towards tested compounds. In our studies, this effect of compound 5b could be correlated to results obtained from cell cycle analysis, wherein HeLa cells were observed to undergo G2/M phase arrest after 48 h as compared to MIA PaCa-2 cells, where similar effect was observed in as early as 12–24 h. Further, less sub G1/Go cells were observed in HeLa cells (Supplementary Fig. S4), indicated lower population of apoptotic cells, as compared to MIA PaCa-2 cells. Although, these observations may provide reasonable explanation for the selectivity of tested compounds towards MIA PaCa-2 cells, but further studies are required to provide a precise mechanism.

Apoptosis is one of the major pathways that lead to the process of cell death. Therefore, it was considered of interest to investigate the apoptosis inducing effect of compound 5b. The results showed significant apoptotic induction in MIA PaCa-2 cells at its IC_{50} (Fig. 2A). Another commonly used method to detect apoptosis is *in situ* detection of DNA fragments, which are the end products of apoptotic signaling cascade, using TUNEL system [13]. Treatment of MIA PaCa-2 cells with compound 5b for 48 h resulted in the incorporation of fluorescein-12-dUTP into terminal 3′-OH groups of fragmented DNA, indicating that apoptotic DNA fragments developed after compound 5b treatment. Further, agarose gel

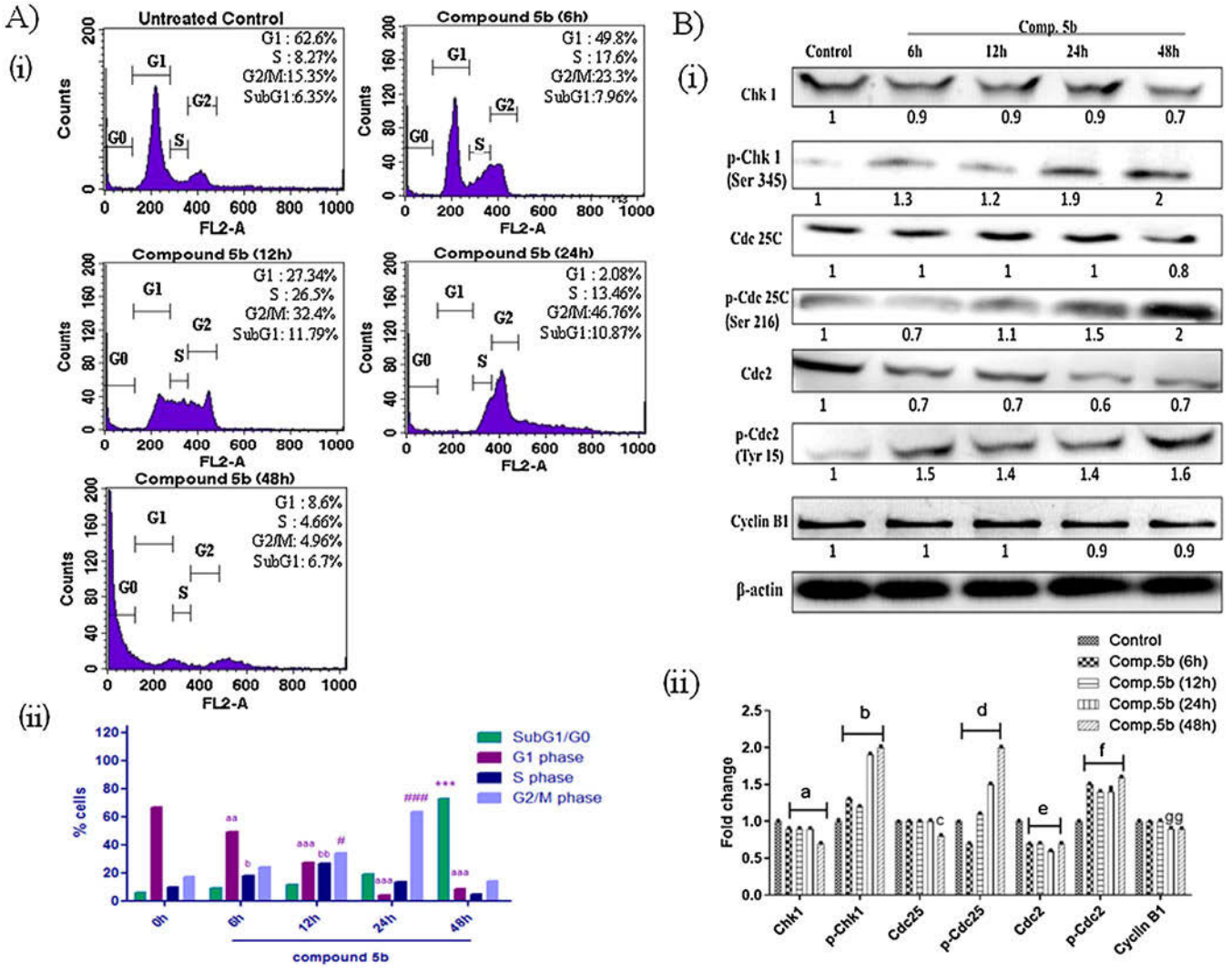

Fig. 5. Compound 5b induced G2/M cell cycle arrest in MIA PaCa-2 cells (A) FACS analysis of DNA distribution in MIA PaCa-2 cancer cells at time intervals of 6, 12, 24 and 48 h, after treatment with compound 5b at its IC_{50}. (ii) Graph bars show the percentage of cells in SubG1/G0, G1, S, and G2/M phases at different time intervals. Data are presented as mean values ± SEM, $n = 3$. Significant differences from respective controls are as follows: $^{*}p < 0.001$; $^{aa}p < 0.01$, $^{aaa}p < 0.001$; $^{b}p < 0.05$, $^{aa}p < 0.001$ and $^{\#}p < 0.05$, $^{\#\#\#}p < 0.001$ (B) Effect of compound 5b on the expression levels of cell cycle proteins associated with G2/M phase arrest in MIA PaCa-2 cells. β-actin was taken as loading control. Graph bars show the fold change in the expression levels of cell cycle proteins at different time intervals (mean ± SEM, $n = 3$). Significant differences from respective controls are as follows: $^{a}p < 0.001$; $^{b}p < 0.001$, $^{c}p < 0.001$; $^{d}p < 0.001$; $^{e}p < 0.001$, $^{f}p < 0.01$ and $^{g}p < 0.001$.

electrophoresis of pooled DNA extracts confirmed that compound 5b caused internucleosomal DNA fragmentation. Taken together, these findings support the contention that compound 5b triggers apoptosis of MIA PaCa-2 cells.

Oxidative stress is implicated in a number of pathological processes including apoptosis, and many chemotherapeutic agents are known to induce their cytotoxic effects on tumor cells by a ROS-mediated mechanism [2,3]. Sulfur containing compounds like disulfides and polysulfides are considered as strong reducing agents which react rapidly with oxidants, such as dioxygen and oxyhaemoglobin, to form reactive oxygen species (ROS), such as the superoxide radical anion ($O_2^{\bullet -}$) and hydrogen peroxide (H_2O_2) [16,17]. Accumulating evidences have also shown that DADS induces apoptosis through the production of H_2O_2 [18]. The present studies revealed that compound 5b promoted intracellular ROS production in MIA PaCa-2. Interestingly, NAC, an antioxidant, was able to alleviate compound 5b-induced ROS generation and cell death in MIA PaCa-2 cells, indicating the involvement of ROS in compound 5b-induced apoptosis in cancer cells. Furthermore, pre-treatment of NAC with compound 5b, significantly abrogated apoptosis (Supplementary Fig.S5), confirming that ROS production is indispensable to the apoptotic action of compound 5b.

Mitochondria plays an essential role in the propagation of apoptosis and its dysfunction is often associated with loss or depolarization of MMP, which leads to collapse of mitochondrial functions ensuing cell death [12]. The decline in MMP (-ΔΨm) revealed that the apoptosis induced by compound 5b might be triggered by alteration of MMP by ROS. Subsequently, attenuation of MMP initiates mitochondrial dependent intrinsic pathway which was confirmed by down-regulation of the Bcl-2/Bax protein ratio, increase in total cytochrome c levels and increase in expression of cleaved caspase-3 proteins in compound 5b treated MIA PaCa-2 cells. Cells have specialized responses to DNA damage that arrest the progression of the cell cycle and facilitate the repair process. In response to DNA damage, checkpoint kinase 1 (Chk1) gets specifically phosphorylated at Serine 345 (S345) and interacts with many downstream effectors to induce G2/M cell cycle arrest. Primarily, the accumulation of phosphorylated Chk1 (p-Chk1) subsequently, phosphorylates Cdc25C at Ser216 residue, which

results in its proteasomal degradation [19]. The degradation has an inhibitory effect on the formation of cyclin-dependent kinase complexes *i.e.* Cdc2/Cyclin B1, which are key drivers of G2/M transition [20]. The present study shows that compound 5b treatment inhibited G2/M phase progression in MIA PaCa-2 cells, in association with the increased expression of phosphorylated forms of Chk-1, Cdc25C and Cdc2 proteins. Taken together the increased expression of phosphorylated Chk1 (p-Chk1) on compound 5b treatment and implication of ROS in cell death by causing DNA damage-induced cell cycle arrest in cancer cells [21], it can be inferred that DNA damage is due to increased ROS levels. The above findings were also consistent with earlier reported studies of DADS, which showed that DADS-induced G2/M checkpoint response was mediated through the ATR/Chk1/Cdc25C/Cyclin B1 pathway [22].

However, polysulfides such as DADS were reported to exert the anti-proliferative action by disarrangement of the cytoskeleton [23] which may generate same pattern of alterations (as observed in current studies). Moreover, NAC has also been proved as a direct competitor with diallyl polysulfides in preserving thiols oxidation and inhibition of microtubule disarrangement. Therefore, it would be worth to inquire if the cell death by DADS analogs involves more than one pathway, by investigating the effect of DADS derivatives on cytosketeletal pathway in future, to further delineate their mechanism of action. In conclusion, this study is the first to demonstrate the *in vitro* therapeutic effect of DADS derivatives on human cancer cell lines, including MIA PaCa-2, HepG2 and HeLa. Moreover, it was evident from the results that anti-cancer activity of DADS analogs was better than the parent compound, DADS. The most potent analog, Bis[3-(3-flourophenyl) prop-2-ene]disulfide (compound 5b), exhibited antitumor effects by inducing ROS generation and subsequently, cancer cell apoptosis and G2/M phase arrest in MIA PaCa-2 cells.Further studies are required to determine detailed cytotoxic mechanism and pharmacokinetic/pharmacodynamic properties of these compounds. The results should expand the scope for further investigation to achieve promising chemotherapeutic agents for cancer treatment.

Conflict of interest

The authors report no conflicts of interest to disclose.

Funding

This work was financially supported by the research grant received from University of Delhi, Delhi, India.

Acknowledgements

The authors wish to gratefully acknowledge scientific contributions from Prof. Vani Brahmachari. Financial assistance from the University of Delhi is acknowledged. The author Vikas Saini wishes to acknowledge the Senior Research Fellowship awarded by the University Grants Commission – Govt. of India. The facilities provided by ACBR and the University of Delhi are gratefully acknowledged.

Appendix A. Supplementary data

Supplementary data associated with this article can be found, in the online version, at http://dx.doi.org/10.1016/j.pharep.2017.03.006.

References

[1] Torre LA, Bray F, Siegel RL, Ferlay J, Lortet-Tieulent J, Jemal A. Global cancer statistics, 2012. CA Cancer J Clin 2015;65(2):87–108.
[2] Trachootham D, Alexandre J, Huang P. Targeting cancer cells by ROS-mediated mechanisms: a radical therapeutic approach? Nat Rev Drug Discov 2009;8(7):579–91.
[3] Wang J, Yi J. Cancer cell killing via ROS: to increase or decrease, that is the question. Cancer Biol Ther 2008;7(12):1875–84.
[4] Nakagawa H, Tsuta K, Kiuchi K, Senzaki H, et al. Growth inhibitory effects of diallyl disulfide on human breast cancer cell lines. Carcinogenesis 2001;32(6):891–7.
[5] Hong YS, Ham YA, Choi JH, Kim J. Effects of allyl sulfur compounds and garlic extract on the expression of Bcl-2, Bax, and p53 in non small cell lung cancer cell lines. Exp Mol Med 2000;32(3):127–34.
[6] Bottone Jr. FG, Baek SJ, Nixon JB, Eling TE. Diallyl disulfide (DADS) induces the antitumorigenic NSAID-activated gene (NAG-1) by a p53-dependent mechanism in human colorectal HCT 116 cells. J Nutr 2002;132(4):773–8.
[7] Manral A, Saini V, Meena P, Tiwari M. Multifunctional novel diallyl disulfide (DADS) derivatives with β-amyloid reducing, cholinergic, antioxidant and metal chelating properties for the treatment of Alzheimer's disease. Bioorg Med Chem 2015;23(19):6389–403.
[8] Sharma M, Tiwari M, Chandra R. Bis [3-(4′-substituted phenyl) prop-2-ene] disulfides as a new class of antihyperlipidemic compounds. Bioorg Med Chem Lett 2004;14(21):5347–50.
[9] Rai SK, Sharma M, Tiwari M. Synthesis, DNA binding, and cytotoxic evaluation of new analogs of diallyldisulfide, an active principle of garlic. Bioorg Med Chem 2008;16(15):7302–10.
[10] Sharma DK, Manral A, Saini V, Singh A, Srinivasan BP, Tiwari M. Novel diallyldisulfide analogs ameliorate cardiovascular remodeling in rats with L-NAME-induced hypertension. Eur J Pharmacol 2012;691(1–3):198–208.
[11] Myeong JC, Young SS, Kee JL. Synthesis of symmetric diallyl disulfides from baylis-Hillman acetates. Bull Korean Chem Soc 200627(11).
[12] Lancelot S, McLean Louis C, Genevieve BM, Lincoln P. Antiproliferative effect induced by novel imidazoline S43126 in PC12 cells is mediated by ROS, stress activated MAPKs and caspases. Pharmacol Rep 2014;66(6):937–45.
[13] Stathopoulou PG, Galicia JC, Benakanakere MR, Garcia CA, Potempa J, Kinane DF. Porphyromonas gingivalis induce apoptosis in human gingival epithelial cells through a gingipain-dependent mechanism. BMC Microbiol 2009;9(1):1.
[14] Yi L, Su Q. Molecular mechanisms for the anti-cancer effects of diallyl disulfide. Food Chem Toxicol 2013;57:362–70.
[15] Powolny AA, Singh SV. Multitargeted prevention and therapy of cancer by diallyl trisulfide and related Allium vegetable-derived organosulfur compounds. Cancer Lett 2008;269(2):305–14.
[16] Munday R, Munday JS, Munday CM. Comparative effects of mono-, di-, tri-, and tetrasulfides derived from plants of the Allium family: redox cycling in vitro and hemolytic activity and phase 2 enzyme induction in vivo. Radic Biol Med 2003;34(9):1200–11.
[17] Chatterji T, Keerthi K, Gates KS. Generation of reactive oxygen species by a persulfide (BnSSH). Bioorg Med Chem Lett 2005;15(17):3921–4.
[18] Kwon KB, Yoo SJ, Ryu DG, Yang JY, Rho HW, Kim JS, et al. Induction of apoptosis by diallyl disulfide through activation of caspase-3 in human leukemia HL-60 cells. Biochem Pharmacol 2002;63(1):41–7.
[19] Daugas E, Susin SA, Zamzami N, Ferri KF, Irinopoulou T, Larochette N, et al. Mitochondrio-nuclear translocation of AIF in apoptosis and necrosis. FASEB J 2000;14(5):729–39.
[20] Reinhardt HC, Yaffe HB. Kinases that control the cell cycle in response to DNA damage: Chk1, Chk2, and MK2. Curr Opin Cell Biol 2009;21(2):245–55.
[21] Caparelli ML, O'Connell MJ. Regulatory motifs in Chk1. Cell Cycle 2013;12(6):916–22.
[22] Ling H, Wen L, Ji XX, Tang YL, He J, Tan H, et al. Growth inhibitory effect and Chk1-dependent signaling involved in G2/M arrest on human gastric cancer cells induced by diallyl disulfide. Braz J Med Biol Res 2010;43(3):271–8.
[23] Xiao D, Pinto JT, Gundersen GG, Weinstein IB. Effects of a series of organosulfur compounds on mitotic arrest and induction of apoptosis in colon cancer cells. Mol Cancer Ther 2005;4:1388–98.